DETECTION AND CLASSIFICATION OF RED BLOOD CELLS ABNORMALITY USING FASTER R-CNN AND GRAPH CONVOLUTIONAL NETWORKS

Amirullah Andi Bramantya[1)], Chastine Fatichah[2)], and Nanik Suciati[3)]
[1, 2, 3)]Department of Informatics, Faculty of Intelligent Electrical and Information Technology
Institut Teknologi Sepuluh Nopember
Sukolilo, Surabaya
e-mail: amirullahandi91@gmail.com[1)], chastine@if.its.ac.id[2)], nanik@if.its.ac.id[3)]

ABSTRACT

Research in medical imagery field such as analysis of Red Blood Cells (RBCs) abnormalities can be used to assist laboratory's in determining further medical actions. Convolutional Neural Networks (CNN) is a commonly used method for the classification of RBCs abnormalities in blood cells images. However, CNN requires large number of labeled training data. A classification of RBCs abnormalities in limited data is a challenge. In this research we explore a semi-supervised learning using Graph Convolutional Networks (GCN) to classify RBCs abnormalities with limited number of labeled sample images. The proposed method consists of 3 stages, i.e., extraction of Region of Interest (ROI) of RBCs from blood images using Faster R-CNN, abnormality labeling and abnormality classification using GCN. The experiment was conducted on a publicly accessible blood sample image dataset to compare classification performance of pretrained CNN models (Resnet-101 and VGG-16) and GCN models (Resnet-101 + GCN and VGG-16 + GCN). The experiment showed that the GCN model build on VGG-16 features (VGG-16 + GCN) produced the best accuracy of 95%.

***Kata Kunci**: Red Blood Cells, Detection, Classification, Faster R-CNN, GCN.*

DETEKSI DAN KLASIFIKASI ABNORMALITAS SEL DARAH MERAH MENGGUNAKAN FASTER R-CNN DAN *GRAPH CONVOLUTIONAL NETWORKS*

Amirullah Andi Bramantya[1)], Chastine Fatichah[2)], and Nanik Suciati[3)]
[1, 2, 3)]Departemen Teknik Informatika, Institut Teknologi Sepuluh Nopember
Sukolilo, Surabaya
e-mail: amirullahandi91@gmail.com[1)], chastine@if.its.ac.id[2)], nanik@if.its.ac.id[3)]

ABSTRAK

Penelitian dalam bidang citra medis seperti analisis abnormalitas Sel Darah Merah dapat digunakan untuk membantu Analis dalam penentuan tindakan medis lanjutan. Metode Convolutional Neural Networks (CNN) merupakan metode yang umum digunakan untuk klasifikasi abnormalitas Sel Darah Merah (Red Blood Cells/RBCs) pada citra sel darah. Namun penerapan dari metode CNN ini memerlukan data label yang cukup besar sebagai data pelatihan. Penelitian klasifikasi abnormalitas dari sel darah merah dengan hasil yang baik pada data yang terbatas merupakan suatu tantangan. Penelitian ini menggunakan semi-supervised learning yang didapatkan dari metode Graph Convolutional Networks (GCN) dimana dengan data sampel darah yang terbatas. Penelitian ini memiliki 3 tahap, yakni pengambilan Region of Interest (ROI) RBCs dari citra sampel darah menggunakan Faster R-CNN, labelisasi abnormalitas dan klasifikasi abnormalitas menggunakan GCN. Uji coba dilakukan pada dataset citra sampel darah yang dapat diakses secara publik dengan membandingkan performa klasifikasi pretrained model CNN (Resnet-101 dan VGG-16) dan model GCN (Resnet-101 + GCN dan VGG-16 + GCN). Hasil pengujian menunjukkan bahwa model GCN yang menggunakan arsitektur VGG16 (VGG16 + GCN) mendapatkan hasil yang sangat baik yakni 95%

***Keywords**: Sel Darah Merah, Deteksi, Klasifikasi, Faster R-CNN, GCN.*

I. INTRODUCTION

IN medical, machine learning is used to solve medical problem, such as medical images in laboratory, MRI, X-Ray, etc [1] - [7]. In medical laboratory, many works using microscopic images which the sample is taken from body part, mainly topic is about bloods. Bloods is a main fluid system that flows to heart, artery and other body parts [8]. Blood cells is a very important part because there's many important information can be researched. In human's life, blood cells continuously growth comparable with human growth. Blood cells consist

of three main cells, which is Red Blood Cells (RBCs), White Blood Cells (WBCs) and platelets where the biggest volume is RBCs.

RBCs classification is an important medical decision to classify the normal and the abnormal one. Generally, shape of RBCs is rounded in top and concave in it's edge with 7.5 μm and 2 μm thickness [9]. Some research about RBCs classification by its shape, to identify its core, and to counting or intensity of RBCs [2] [10]. RBCs abnormality can signify about patient condition, such as anemia [2] [10]. Some example of RBCs abnormalities is spherocyte, codocyte, stomatocyte, ovalocyte, elliptocyte, degmacyte, drepanocyte, dacrocytes, acanthocyte and echinocyte. The problem in manual classification can make laboratory became fatigue and the classification can make wrong result [3] [8].

For RBCs classification, common method that used is CNN. There's large labeled data that used in CNN training, when small data makes the result is not too good [11]. In real world, when there's small labeled data, labeling other data is a challenge. To handle the data deficiency, one of CNN development is using Graph Convolutional Networks (GCN) that use graph structure relation between nodes with feature points during its aggregation [12]. Graph or networks is a data structure that consists of nodes (vertices) and relation between nodes (edges) likes social networks, references networks, biology protein interaction, etc [13]. GCN is developed because conventional CNN is not possible to analyze non-Euclidean that resulting from graph structure of feature maps [5]. In GCN, method input consists of graph representation of feature maps that resulted from CNN layer. Main theory that used is GCN learning is semi-supervised learning, this method is capable to labeling unlabeled data with small labeled data during training [12]. Some GCN that use in medical images such as Alzheimer classification [12] [5], cervical cancer cell classification [14]. Research with GCN using training phase less than 70% available data resulted that its better than CNN conventional with larger training data [14] [6].

In context of Alzheimer disease, a neurodegenerative disorder associated with network dysfunction. Then a graph-based tools is very important to get significant complexity in brain connectivity studies [6]. Graph-based that is non-Euclidean domain is similar with brain connectivity. It shows that graph is capable to find a connection between brain points. CNN based that used as data representation and classification can be used in graph-based neighborhood definition, or in the same dimension. With limited existing data of one point, the assumption of similarity with another pint can be explored.

In classification of cervical cell is an important prevention against cancer. Early stages detection of cell is a basic method for medical personnel get advanced examination. Limited existing data of cervical cell that presented in real world is one of preventive weakness [14]. To handle lack of labeled data in large dataset, relation between data is proposed using semi-supervised learning to find a relation between data. Data or images is processed using CNN architecture to generate its feature maps. In same dimension, the similarity between feature maps can be used to calculate similarity between images. In data that represented as graph relation can be classified with limited labeled data [15]. Classification of nodes in graph where the labeled data is small can be framed as semi-supervised learning, where the label information is connected between nodes in the same dimension.

This paper organized as Section II describes theories that used in this research, Section III explains whole method that used in this research, Section IV explains the discussion of the result and the comparison with other method. Finally conclusion and future works are presented in Section V.

II.LITERATURE STUDY

Some research in computer vision about blood cells abnormality using image processing and Wiener filter and Sobel edge detection, Support Vector Machine (SVM) is capable to identify RBCs shape and size variations [9] [10]. Identification of WBCs abnormality by counting its intensity to identify another disease by WBCs amount [16]. In RBCs there's some research about RBCs abnormalities classification, improvement of RBCs abnormality detection using image processing [17] that using improved Decision-Tree Algorithm [8], deep learning method using AlexNet [18], Deep Learning and SVM [3], sub-type of blood cells classification using CNN [11].

In this research, first thing to do is identify ROI of each blood cells. Faster R-CNN is proposed for detection of blood cells. Faster R-CNN works using VGG-16 feature maps extraction, the feature maps is processed into Region Proposal Networks (RPN) to identify if there's a proposed object in the area/region. Then, in the proposed region, Region of Interest (RoI) method is used to calculate if there's object in the region. The result of Faster R-CNN is a bounding boxes with class of the object. Then the detected RBCs or its ROI is extracted into single cell. The RBCs ROI images is used as a groundtruth for CNN classification training.

Then, laboratory expert classifies identified RBCs ROI images into abnormality classes. In this research 3 RBCs abnormality classes is detected and used, there's ovalocyte, stomatocyte and cigar. Then, images is resized into 224 x 224 pixels in RGB format, then augmented by rotating and flipping the images. To classify the RBCs abnormality, GCN method is proposed as classifier. GCN model combined graph structure and feature maps, then distributed through graph using convolution layer.

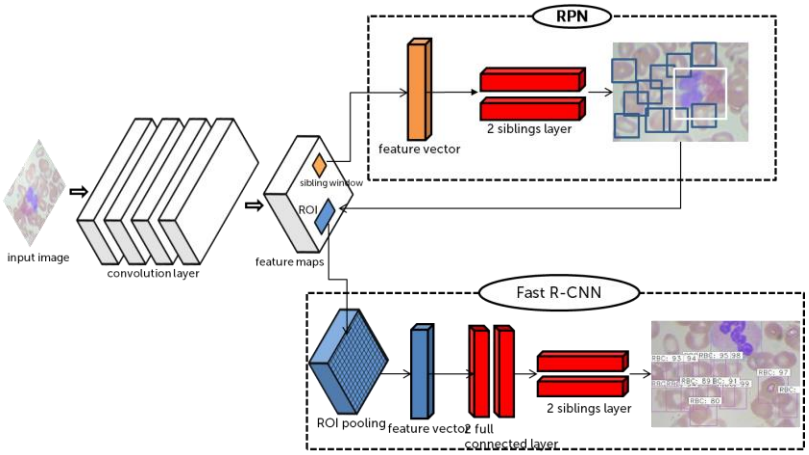

Figure 1. Faster R-CNN.

A. Faster R-CNN

The first purpose in this research is to identify RBCs images from BCCD Dataset. One of deep learning method that capable to do this is Faster R-CNN as shown in Figure 1. Faster R-CNN. Faster R-CNN is one of CNN method that developed from Fast R-CNN, which consist of 2 modules. First, deep fully convolutional networks that propose a region from an RPN and Fast R-CNN module that use the proposed region, then both modules using same proposed region. Main system in Faster R-CNN is an RPN module that taking images as input and the output is an object with its bounding box.

First step of Faster R-CNN is RPN module is extracting feature maps from images using VGG-16 module. Then the feature maps is processed using identical fully connected layer that consist of box-regression layer and box-classification layer. For each sliding window, there's many proposed region that may lie an object in it, that called anchors. Anchors is positioned in the center of sliding window with size 3x3, for each sliding window there's 9 anchors with 3 scale size and 3 ratio (1:1, 1:2, 2:1). Second step is Fast R-CNN module that use to classify object proposal that detected by RPN. Fast R-CNN get an input from images feature maps and object proposal collection from RPN. Then each object is mapped into ROI and processed using identical fully connected layer using softmax classifier. The result of Faster R-CNN is bounding box and the class of the object.

B. Data Augmentation

Dataset in machine learning is one of important parts. If the provided dataset is very small in the training, the result accuracy will not good enough than more varied datasets. Furthermore, the accuracy may resulted not good enough. Its essential to provide more data variety from the provided dataset, then data augmentation is needed to solve this problem. The data augmentation method that used in this research are vertical flip, horizontal flip and rotating. The result of is a more varied images, thus the image characteristic is better during the training process. The CNN method then use this varied image dataset during training phase. Then, the augmented image is classified by expert to get its abnormality class. In this research, there's 3 abnormality class by RBCs shape is detected there's cigar cell, ovalocyte and stomatocyte. The augmented images with abnormality class then use as CNN ground truth.

C. Graph Convolutional Networks (GCN)

Graph Convolutional Networks is one of deep learning method that combining between graph relation and CNN. GCN is a representation of conventional CNN where input of the neural networks implicitly as a graph. GCN consist of few convolutional layers to get feature maps representation as shown in Figure 2. Main idea of GCN is to represent nodes or vertices with feature X and other features. Conventional Graph theory that represented in (1). Where V is nodes or vertices and E is edge or relation between nodes. Nodes in graph has a feature that represented as X, where $X \in R^{n \times d}$ is a matrix of vertices and $X_v \in R^d$ describe feature of vertices v.

$$G = (V, E), \tag{1}$$

GCN using feature maps representation of each nodes in graph, where the relation of each nodes is using Laplacian Adjacency matrix. First is using Euclidean Adjacency matrix from distance between each feature maps. GCN function form in where the input is a feature x_i for every node i, that represented in (2)

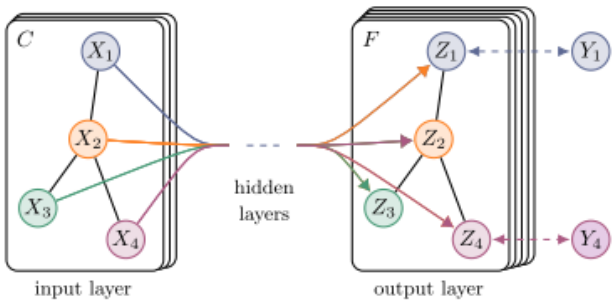

Figure 2. GCN.

$$N \times D, \tag{2}$$

$$A_{ij} = \begin{cases} 1\ e_{ij} \in E, \\ 0\ e_{ij} \notin E. \end{cases} \tag{3}$$

Where N is a nodes amount and D is an input features. In (2) then represented as an adjacency matrix. Adjacency matrix (A) is a relation between nodes in $n \times n$ matrix, where A is defined in (3).

$$g_\theta * X \approx \theta\left(I_N + D^{-\frac{1}{2}}AD^{-\frac{1}{2}}\right)X. \tag{4}$$

Convolutional layer of CNN feature maps using Chebyshev polynomial that described in (4). Where * is convolution operator and I_N is matrix dimension and D is a diagonal matrix. For every neural network is defined as non-linear function that described in (4). This also represent H in each layer.

$$H^{(l+1)} = f\left(H^{(l)}, A\right). \tag{5}$$

Where in $H^{(0)} = X$ and $H^{(l)} = Z$, Z is a layer output and l is a layer level. GCN is following the rule of layer propagation that described in (5), where A is substituted by Chebysev polynomial.

$$H^{(l+1)} = \theta\left(\tilde{D}^{-\frac{1}{2}}\tilde{A}\tilde{D}^{-\frac{1}{2}}H^{(l)}W^{(l)}\right). \tag{6}$$

$\tilde{A} = A + I_N$ is symmetrical normalized Laplacian adjacency matrix that described from (6).

$$L^{sym} := D^{-\frac{1}{2}}LD^{-\frac{1}{2}} = I - D^{-\frac{1}{2}}AD^{-\frac{1}{2}}. \tag{7}$$

With $H^{(l)}$ as an convolution matrix on layer-l, then in layer $H^{(0)}$ where the known parameter only X and A then described as (7). In this research, there's 2 GCN layer for classification that simplified using softmax classifier that described in (9).

$$H^{(0)} = X, \widetilde{A} = A + I_N, \widetilde{D} = \sum_j \tilde{A}_{ij,} W^{(l)} \tag{8}$$

$$Z = f(X, A) = \text{softmax}\left(\hat{A}\,\text{ReLU}\left(\hat{A}XW^{(0)}\right)W^{(1)}\right) \tag{9}$$

III.METHODOLOGY

The research is consisted into 3 phases, detection of RBCs ROI using Faster R-CNN, labeling and data augmentation, classification of RBCs abnormality using GNN as shown in Figure 3. To identify RBCs images from blood samples, Faster R-CNN is used to identify blood classes because its capable to identify multi-class from images. The result of Faster R-CNN is type of blood parts such as RBCs, WBCs and platelets, but only RBCs images is used in this research. Dataset in this research is BCCD Dataset that available to accessed publicly.

A. Dataset

Dataset that use in this research that consist of 4888 label with 3 classes, there Red Blood Cells (RBCs), White Blood Cell (WBCs) and Platelets as shown in Figure 4. This dataset consist of 364 images with size of each image is 640 x 480 pixels. Then the CSV file as annotation data and Faster R-CNN ground truth. Bounding box of Annotation data form each class in BCCD Dataset as shown in TABLE I. In this research, only RBCs images is use for research object.

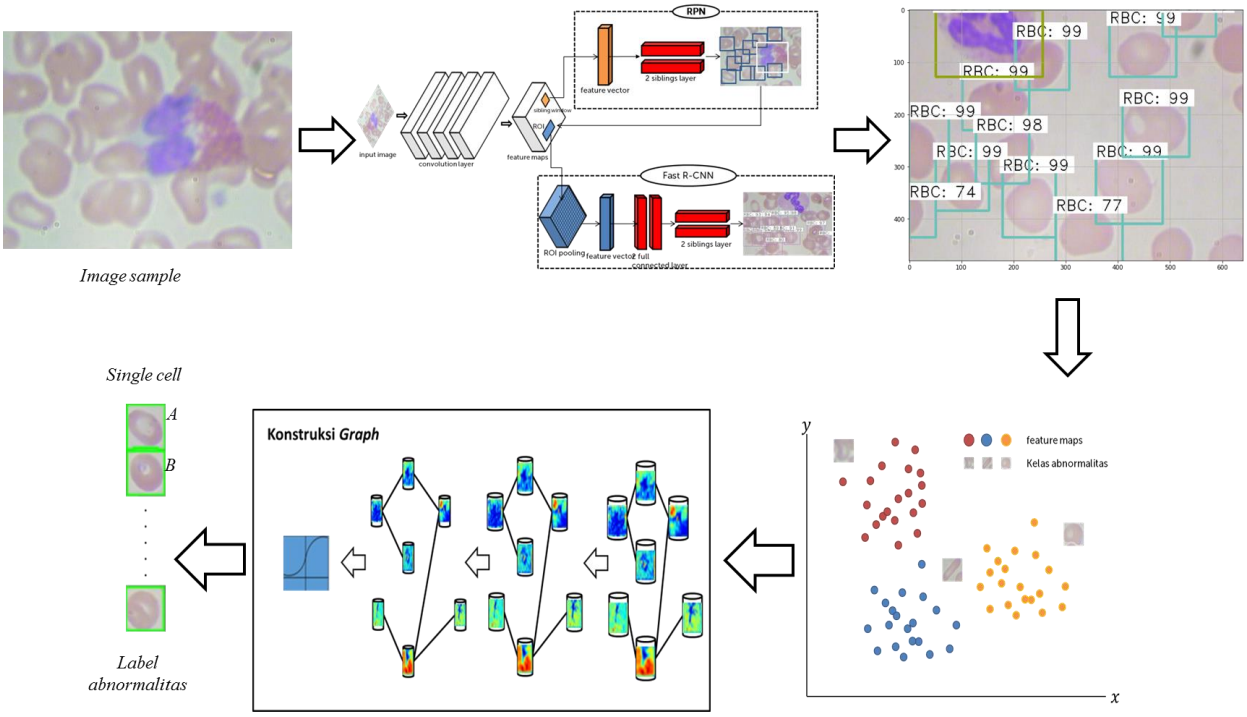

Figure 3. Proposed Research.

TABLE I
BCCD DATASET

Blood Class	Total Data
Red Blood Cells	3757
White Blood Cells	335
Platelets	361

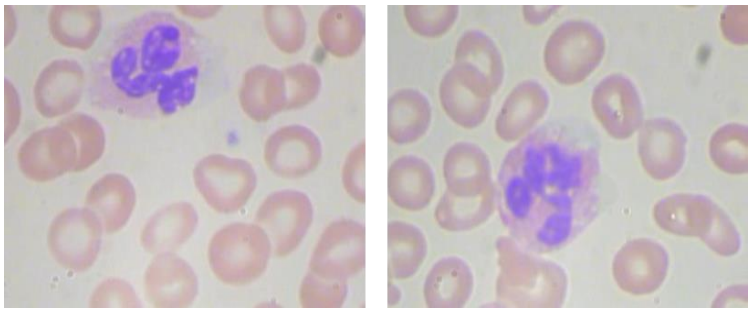

Figure 4. BCCD Dataset.

B. Result of Faster R-CNN

In ROI RBCs extraction from BCCD Dataset using Faster-RCNN, training phase using 294 images and 36 images as testing. In training phase, there's 294 platelets, 2938 RBCs and 263 WBCs. Using training parameter 40.000 batches, the accuracy of Faster R-CNN is 80%, training result of Faster R-CNN is shown in Figure 5. This model training shows descending graph that shows good result in loss regression during training and the accuracy in ascending graph shows the accuracy is getting better during training.

Result of Faster R-CNN is an image is a ROI of BCCD blood cells class with its bounding boxes. ROI is extracted to get single cell images and grouped into each class as shown in Figure 6. Another purpose using Faster R-CNN in to make greater data, because there's additional extracted ROI from same images. The result is shown in Figure 7, there's additional 4 RBCs ROI that detected. Faster R-CNN evaluation using mean average precision (mAP), that comes from average result of class precision in each image. From 36 images mAP from all class is 71%, and mAP from each class also shown in Figure 8.

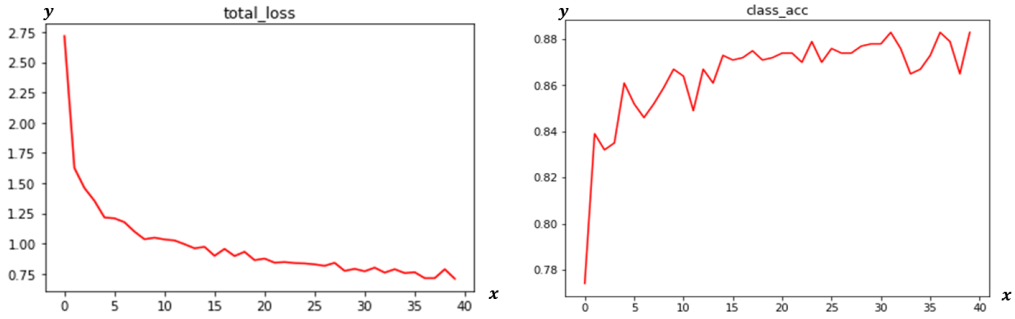

Figure 5. Loss and Accuracy Graph.

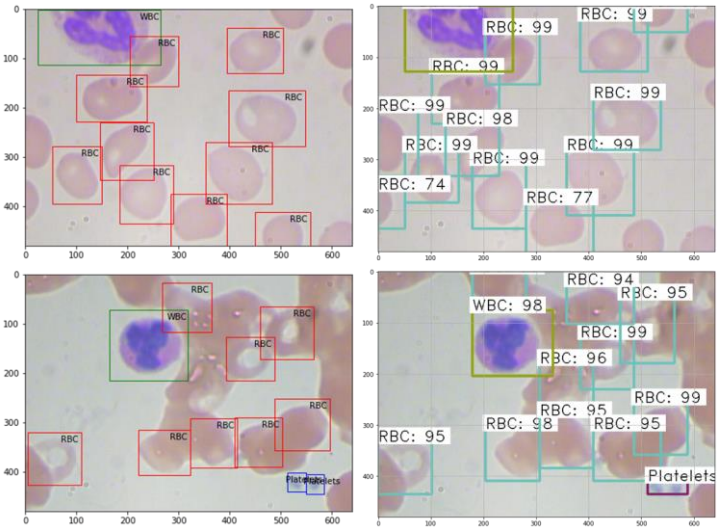

Figure 6. Faster R-CNN Comparison Result.

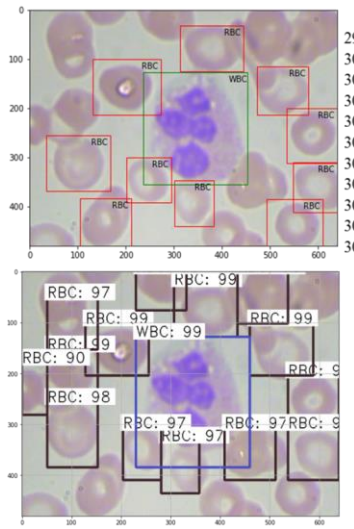

	filename	class	xmin	ymin	xmax	ymax
2999	BloodImage_00334.jpg	RBC	201	300	295	392
3000	BloodImage_00334.jpg	RBC	301	346	382	439
3001	BloodImage_00334.jpg	RBC	535	199	640	312
3002	BloodImage_00334.jpg	RBC	131	100	272	213
3003	BloodImage_00334.jpg	RBC	35	254	167	368
3004	BloodImage_00334.jpg	RBC	493	385	610	480
3005	BloodImage_00334.jpg	RBC	313	31	445	125
3006	BloodImage_00334.jpg	RBC	104	383	211	480
3007	BloodImage_00334.jpg	RBC	472	114	580	213
3008	BloodImage_00334.jpg	RBC	548	310	640	411
3009	BloodImage_00334.jpg	WBC	236	126	453	355

class	prob
'RBC'	99.70129
'RBC'	99.6484
'RBC'	99.53824
'RBC'	99.30128
'RBC'	99.18771
'RBC'	98.8663
'RBC'	98.43094
'RBC'	97.91668
'RBC'	97.74499
'RBC'	97.67284
'RBC'	97.4674
'RBC'	96.53855
'RBC'	90.79214
'RBC'	90.10986
'WBC'	99.90344

Figure 7. Faster R-CNN ROI Result Comparison.

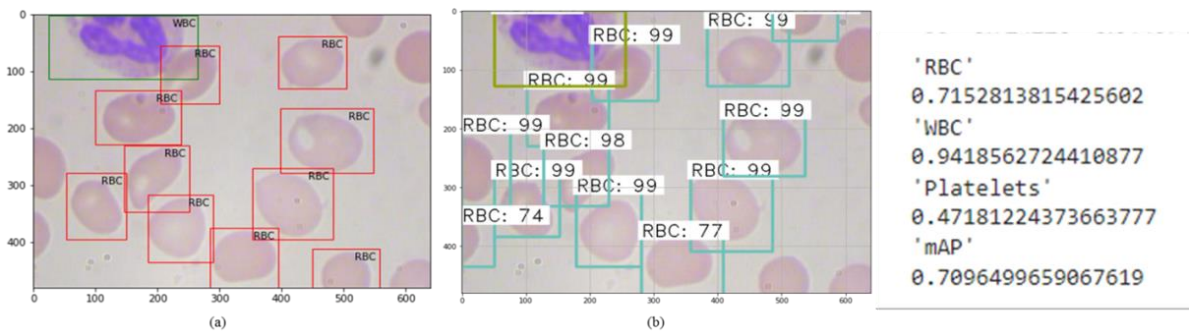

Figure 8. Faster R-CNN mAP.

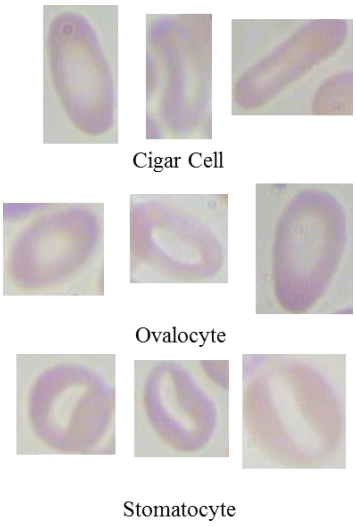

Figure 9. Abnormality Class.

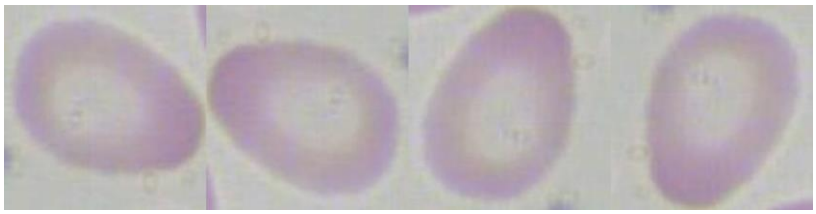

Figure 10. Data Augmentation Result.

C.Data Augmentation

Images that used in this research only RBCs RO, then the image is classified by pathology expert to get it's abnormality class. In this research, there's 3 abnormality RBCs class is used, stomatocyte, ovalocyte and cigar as shown in Figure 9. Then, the images is resized into 224x224 pixels size. Because the images in each class is not too much, data augmentation method is proposed to generate more data for training purpose. There's a few data augmentation method that used in this research, there's horizontal flipping, vertical flipping and rotation for 90^{o}, 180^{o} and 270^{o}. The result of data augmentation as shown in Figure 10.

D. Classification using GCN

In this research, there's 2 CNN architecture that use as feature maps extraction (Resnet-101 and VGG-16). In this research, input of GCN is no longer an image but a feature maps data. In Resnet-101, layer that use is avg_pool layer, this layer placed just before prediction layer. In this layer, there's 2048 feature maps, that represented in Figure 11 from each abnormality class.

	0	1	2	3	...	2044	2045	2046	2047	class
0	0.402125	0.000000	0.000000	0.000000	...	0.000000	0.000000	0.462871	0.031270	cigar
1	0.345092	0.000000	0.000000	0.000000	...	0.000000	0.000000	0.000000	0.000000	cigar
2	0.840129	0.014244	0.000000	0.000000	...	0.127003	0.000000	0.059988	0.000000	cigar
3	0.758761	0.000000	0.000000	0.000000	...	0.000000	0.010252	0.235732	0.000000	cigar

	0	1	2	3	...	2044	2045	2046	2047	class
0	2.599946	0.000000	0.000000	0.013968	...	0.000000	0.069643	0.200621	0.122302	oval
1	0.512086	0.000000	0.003172	0.000000	...	0.000000	0.019022	0.201070	0.007082	oval
2	2.012377	0.023865	0.019587	0.000000	...	0.001704	0.000000	0.259719	0.000000	oval
3	3.202339	0.282467	0.000000	0.000000	...	0.000000	0.000000	0.090892	0.036225	oval

	0	1	2	3	...	2044	2045	2046	2047	class
0	0.365994	0.225396	0.000000	0.000000	...	0.083335	0.002017	0.170132	0.000000	stomatocyte
1	0.503484	0.138521	0.000000	0.000000	...	0.000000	0.000000	0.082112	0.000000	stomatocyte
2	0.353406	0.023378	0.000000	0.000000	...	0.129351	0.000000	0.005286	0.000000	stomatocyte
3	0.028942	1.166105	0.000000	0.002830	...	0.138522	0.000000	0.132215	0.000000	stomatocyte

Figure 11. Resnet-101 feature maps extraction.

TABLE II
RESNET-101 EUCLIDEAN DISTANCE MATRIX.

	0	1	2	3	4	...	427	428	429	430	431
0	0	27.3618	41.1055	27.1284	25.1336	...	30.433	29.8259	29.0636	27.9812	32.9703
1	27.3618	0	39.1912	29.2767	25.7317	...	33.1156	30.8573	31.8693	32.1041	29.5422
2	41.1055	39.1912	0	36.0489	39.8895	...	38.4908	33.436	38.6957	41.2494	41.8346
3	27.1284	29.2767	36.0489	0	26.1353	...	29.0137	24.4766	28.2241	23.4762	32.8486
4	25.1336	25.7317	39.8895	26.1353	0	...	33.3289	31.0768	32.5787	31.047	33.6544
...	...	...	...	...	...	...	...	...	...	...	...
427	30.433	33.1156	38.4908	29.0137	33.3289	...	0	24.8036	19.0109	31.6844	34.5157
428	29.8259	30.8573	33.436	24.4766	31.0768	...	24.8036	0	26.3004	28.6362	31.624
429	29.0636	31.8693	38.6957	28.2241	32.5787	...	19.0109	26.3004	0	32.3631	33.526
430	27.9812	32.1041	41.2494	23.4762	31.047	...	31.6844	28.6362	32.3631	0	36.6754
431	32.9703	29.5422	41.8346	32.8486	33.6544	...	34.5157	31.624	33.526	36.6754	0

TABLE III
RESNET-101 LAPLACIAN ADJACENCY MATRIX.

	0	1	2	3	4	...	427	428	429	430	431
0	0.977388	0.000062	0.000007	0.000058	0.000077	...	0.000053	0.000056	0.000067	0.000051	0.000027
1	0.000062	0.977888	0.000008	0.000037	0.000075	...	0.000038	0.000046	0.000046	0.000033	0.000050
2	0.000007	0.000008	0.993883	0.000006	0.000009	...	0.000010	0.000010	0.000009	0.000010	0.000010
3	0.000058	0.000037	0.000006	0.657379	0.000046	...	0.000040	0.000065	0.000049	0.000054	0.000020
4	0.000077	0.000075	0.000009	0.000046	0.979215	...	0.000044	0.000050	0.000045	0.000050	0.000029
...	...	...	...	...	...	...	...	...	...	...	...
427	0.000053	0.000038	0.000010	0.000040	0.000044	...	0.979454	0.000112	0.000251	0.000057	0.000031
428	0.000056	0.000046	0.000010	0.000065	0.000050	...	0.000112	0.979395	0.000093	0.000068	0.000034
429	0.000067	0.000046	0.000009	0.000049	0.000045	...	0.000251	0.000093	0.978081	0.000047	0.000035
430	0.000051	0.000033	0.000010	0.000054	0.000050	...	0.000057	0.000068	0.000047	0.981103	0.000022
431	0.000027	0.000050	0.000010	0.000020	0.000029	...	0.000031	0.000034	0.000035	0.000022	0.980513

Feature maps then calculated its distance matrix to each nodes using Euclidean distance, the result is $n\ x\ n$ matrix, where n is nodes amount as shown in TABLE II. In Euclidean distance matrix there's value 0 in its diagonal, shows that distance node by itself is none or 0. GCN constructed using Laplacian Adjacency Matrix that shown in

TABLE III where Laplacian Adjacency matrix also $n\ x\ n$ matrix. In Laplacian matrix shows value in its diagonal close to 1, it shows that similarity of nodes by itself is close enough. On GCN, training, 347 images as training data and 85 images as testing data. Training parameter using 2000 epochs and 0.8 as dropout value.

The other CNN architecture that uses for feature maps extraction is using VGG-16 architecture. in VGG-16, layer that use as feature maps extraction in flatten layer, this layer positioned after max_pooling layer after 5th convolution layer and just before dense layer.in this layer, there's 25088 feature maps that represented in Figure 12. Euclidean distance matrix of VGG-16 feature maps shown in TABLE IV as $n\ x\ n$ matrix and Laplacian Adjacency Matrix for GCN shown in TABLE V.

IV.RESULTS AND DISCUSSION

Result and evaluation of ROI detection with Faster R-CNN, tested parameter is mAP on each blood cells class and mAP for all blood cells class. Result of Faster R-CNN mAP shown in TABLE VI, where mAP in WBCs is highest above all, it may because RBCs ROI looks very different from others. In Faster R-CNN, there's also additional ROI that may be taken as additional images for varied data.

Training accuracy of Resnet-101 and GCN is 71% and testing accuracy is 65% that shown in Figure 13. Confusion matrix of Resnet-101 result shown in

Figure 14, the accuracy of Cigar Cell and Stomatocyte is much better than Ovalocyte. It is because Ovalocyte has smallest data than other classes.

	0	1	2	3	...	25084	25085	25086	25087	class
0	0.283413	0	0.122947	0.079272	...	0.170583	0.048859	0.103416	0	cigar
1	0.300275	0	0.113837	0.077449	...	0.179466	0.05484	0.095607	0	cigar
2	0.294118	0	0.118939	0.078572	...	0.18606	0.042653	0.102834	0	cigar
3	0.264468	0	0.118945	0.07541	...	0.165768	0.044654	0.11752	0	cigar

	0	1	2	3	...	25084	25085	25086	25087	class
0	0.055879	0.043605	0.202195	0.137522	...	0.107318	0	0.260748	0.178644	oval
1	0.066923	0.0592	0.179546	0.153312	...	0.084817	0	0.249031	0.175583	oval
2	0.059574	0.038749	0.208068	0.138284	...	0.102671	0	0.258073	0.187607	oval
3	0.055271	0.0448	0.158575	0.146477	...	0.104583	0	0.278562	0.189085	oval

	0	1	2	3	...	25084	25085	25086	25087	class
0	0.198655	0.086861	0.043321	0.192313	...	0.087175	0.068496	0.253601	0.181659	stomatocyte
1	0.216848	0.110736	0.035003	0.197676	...	0.050862	0.029605	0.189088	0.135368	stomatocyte
2	0.182666	0.091567	0.073257	0.192355	...	0.077252	0.077178	0.235727	0.200981	stomatocyte
3	0.162745	0.064038	0.037517	0.132074	...	0.07266	0.047553	0.229169	0.227627	stomatocyte

Figure 12. VGG-16 feature maps extraction.

TABLE IV
VGG-16 EUCLIDEAN DISTANCE MATRIX

	0	**1**	**2**	**3**	**4**	**...**	**427**	**428**	**429**	**430**	**431**
0	0	2.03931	1.78457	2.90372	3.29125	...	23.6998	23.614	23.7008	24.3162	25.882
1	2.03931	0	2.12355	3.16884	2.96746	...	23.7252	23.5985	23.7245	24.3174	25.8808
2	1.78457	2.12355	0	2.69086	3.28519	...	23.7254	23.6244	23.7182	24.3394	25.8915
3	2.90372	3.16884	2.69086	0	2.75814	...	23.5999	23.5095	23.5872	24.2414	25.8378
4	3.29125	2.96746	3.28519	2.75814	0	...	23.6246	23.4927	23.6038	24.219	25.8296
...	...	...	...	...	...	...	...	...	...	...	...
427	23.6998	23.7252	23.7254	23.5999	23.6246	...	0	5.33505	4.37792	5.58647	5.58392
428	23.614	23.5985	23.6244	23.5095	23.4927	...	5.33505	0	5.30269	5.48424	5.59964
429	23.7008	23.7245	23.7182	23.5872	23.6038	...	4.37792	5.30269	0	5.28927	5.43513
430	24.3162	24.3174	24.3394	24.2414	24.219	...	5.58647	5.48424	5.28927	0	4.10457
431	25.882	25.8808	25.8915	25.8378	25.8296	...	5.58392	5.59964	5.43513	4.10457	0

TABLE V
VGG-16 LAPLACIAN ADJACENCY MATRIX

	0	**1**	**2**	**3**	**4**	**...**	**427**	**428**	**429**	**430**	**431**
0	0.358273	0.008227	0.014957	0.002030	0.001652	...	0.000002	0.000002	0.000002	0.000002	0.000002
1	0.008227	0.358978	0.007370	0.001818	0.001924	...	0.000002	0.000002	0.000002	0.000002	0.000002
2	0.014957	0.007370	0.360348	0.002121	0.001646	...	0.000002	0.000002	0.000002	0.000002	0.000002
3	0.002030	0.001818	0.002121	0.559220	0.006793	...	0.000002	0.000002	0.000002	0.000002	0.000002
4	0.001652	0.001924	0.001646	0.006793	0.572266	...	0.000002	0.000002	0.000002	0.000002	0.000002
...	...	...	...	...	...	...	...	...	...	...	...
427	0.000002	0.000002	0.000002	0.000002	0.000002	...	0.791420	0.003358	0.006075	0.000882	0.000291
428	0.000002	0.000002	0.000002	0.000002	0.000002	...	0.003358	0.792533	0.003430	0.000806	0.000270
429	0.000002	0.000002	0.000002	0.000002	0.000002	...	0.006075	0.003430	0.790706	0.000910	0.000288
430	0.000002	0.000002	0.000002	0.000002	0.000002	...	0.000882	0.000806	0.000910	0.704780	0.000633
431	0.000002	0.000002	0.000002	0.000002	0.000002	...	0.000291	0.000270	0.000288	0.000633	0.759192

Training parameter and dataset used in Resnet-101 are also used in VGG-16. Training accuracy of VGG-16 and GCN is 96% and testing accuracy is 95%, as shown in Figure 15. Accuration testing result of VGG-16 and GCN that shown as confusion matrix in each class shown in Figure 16. In Figure 16 the result in each class it shows good accuracy, it shows that complexity of feature maps extraction may makes better in GCN training.

TABLE VI
Faster R-CNN mAP.

Class	mAP
RBCs mAP	0.7152813815425602
WBCs mAP	0.9418562724410877
Platelets mAP	0.47181224373663777
mAP	0.7096499659067619

Classification Report

	precision	recall	f1-score	support
cigar	0.57	0.65	0.61	26
oval	0.38	0.21	0.27	14
stomatocyte	0.74	0.78	0.76	45
accuracy			0.65	85
macro avg	0.56	0.55	0.55	85
weighted avg	0.63	0.65	0.63	85

Figure 13. Resnet-101 Result.

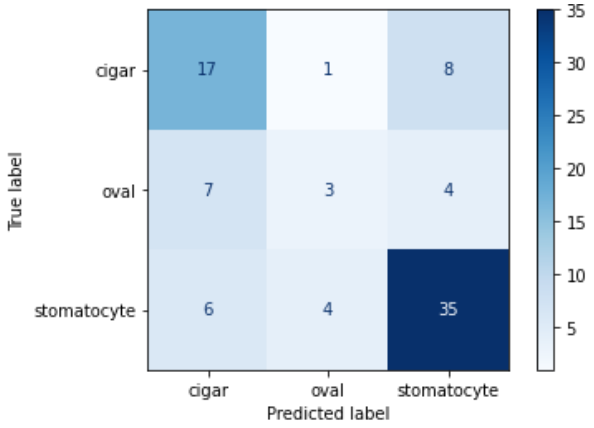

Figure 14. Resnet-101 Confussion Matrix.

Classification Report

	precision	recall	f1-score	support
cigar	0.96	1.00	0.98	26
oval	0.82	1.00	0.90	14
stomatocyte	1.00	0.91	0.95	45
accuracy			0.95	85
macro avg	0.93	0.97	0.95	85
weighted avg	0.96	0.95	0.95	85

Figure 15. VGG-16 Result.

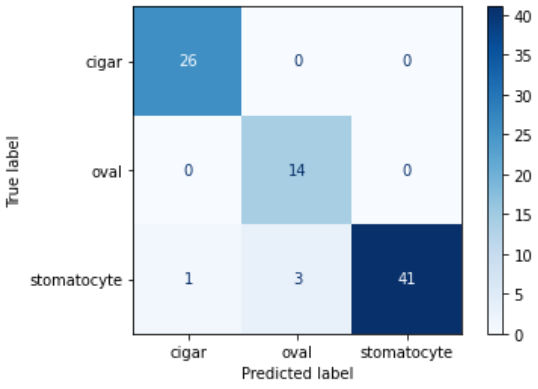

Figure 16 VGG-16 Confusion Matrix.

TABLE VII
Method Result Comparison

Method	Accuracy	Precission	Recall
Resnet-101	0.27	0.25	0.25
VGG-16	0.54	0.33	0.18
Resnet-101 - GCN	0.64705	0.56211	0.54863
VGG-16 - GCN	0.95294	0.92883	0.97037

In this research, proposed method also compared with Resnet-101 and VGG-16 with similar training and testing dataset. In TABLE VII, shows comparison between our method and other CNN method. It shows that out proposed classification method is better than other CNN classification method. Accuracy using Resnet-101 as classification is 27% and 65% in Resnet-101 + GCN and classification using VGG-16 is 54% and 95% using VGG-16 + GCN. Comparison between GCN shows that feature maps extraction using VGG-16 architecture is much higher with than Resnet-101. Complexity of feature maps extraction using VGG-16 likely take effect on nodes identification.

V.CONCLUSION

This research presents a detection of RBCs using Faster R-CNN shows that capability of the Faster R-CNN has a good performance with BCCD Dataset. Faster R-CNN evaluation using mAP shows that 71% for all blood cell class, that consists of 71% for RBCs, 94% of WBCs and 47% of Platelets. During Faster R-CNN, there's some additional images ROI that detected on testing images, it shows that this model is capable to get another ROI that can be use as additional data. RBCs ROI that detected by Faster R-CNN then classified into 3 abnormality class there's Cigar Cell, Ovalocyte and Stomatocyte. Uneven data amount between abnormality class then handled using data augmentation. Data augmentation that proposed mainly use to make more varied data in each class. RBCs ROI then extracted it's feature maps using CNN architecture, in this research using Resnet-101 and VGG-16 architecture. Using Resnet-101 there's 2048 extracted feature maps and 25088 feature maps using VGG-16. Extracted feature maps processed with semi-supervised learning method then classified using GCN. Result of the GCN between both feature maps architecture shows that VGG-16 feature maps has better performance that Resnet-101 feature maps. It may shows that complexity of feature maps extraction may get more detailed data from RBCs ROI, then it can get better similarities values between ROI. Comparison with similar amount of training and testing data using Resnet-101 and VGG-16 as classifier also shows that proposed method using GCN as classifier got better result than original method. Another ROI detection and extraction method may can be used to get additional images to get varied data. Exploration using another feature maps using CNN architecture or using different methods may be use for further research.

REFERENCES

[1] C. Khongkhatithum, P. Kadegasem, W. Sasanakul, L. Thampratankul, A. Chuansumrit, and N. Sirachainan, "Abnormal red blood cell indices increase the risk of arterial ischemic stroke in children," *J. Clin. Neurosci.*, vol. 62, pp. 117–120, 2019.

[2] M. Xu, D. P. Papageorgiou, S. Z. Abidi, M. Dao, H. Zhao, and G. E. Karniadakis, "A deep convolutional neural network for classification of red blood cells in sickle cell anemia," *PLOS Comput. Biol.*, vol. 13, no. 10, p. e1005746, Oct. 2017.

[3] H. A. Aliyu, R. Sudirman, M. A. A. Razak, and M. A. Abd Wahab, "Red blood cells abnormality classification: Deep learning architecture versus support vector machine," *Int. J. Integr. Eng.*, vol. 10, no. 7, pp. 34–42, 2018.

[4] A. M. Patil, M. D. Patil, and G. K. Birajdar, "White Blood Cells Image Classification Using Deep Learning with Canonical Correlation Analysis," *IRBM*, vol. 1, pp. 1–12, 2020.

[5] X. Zhao, F. Zhou, L. Ou-Yang, T. Wang, and B. Lei, "Graph convolutional network analysis for mild cognitive impairment prediction," *Proc. - Int. Symp. Biomed. Imaging*, vol. 2019-April, no. Isbi, pp. 1598–1601, 2019.

[6] T. A. Song *et al.*, "Graph convolutional neural networks for Alzheimer's disease classification," *Proc. - Int. Symp. Biomed. Imaging*, vol. 2019-April, no. Isbi, pp. 414–417, 2019.

[7] A. S. Chowdhury, S. M. Bhandarkar, R. W. Robinson, and J. C. Yu, "Virtual multi-fracture craniofacial reconstruction using computer vision and graph matching," *Comput. Med. Imaging Graph.*, vol. 33, no. 5, pp. 333–342, 2009.

[8] V. M. E. Batitis, M. J. G. Caballes, A. A. Ciudad, M. D. Diaz, R. D. Flores, and E. R. E. Tolentin, "Image Classification of Abnormal Red Blood Cells Using Decision Tree Algorithm," *Proc. 4th Int. Conf. Comput. Methodol. Commun. ICCMC 2020*, no. Iccmc, pp. 498–504, 2020.

[9] P. Rakshit and K. Bhowmik, "Detection of Abnormal Findings in Human RBC in Diagnosing Sickle Cell Anaemia Using Image Processing," *Procedia Technol.*, vol. 10, pp. 28–36, 2013.

[10] C. C. Hortinela, J. R. Balbin, J. C. Fausto, P. Daniel Divina, and J. P. T. Felices, "Identification of Abnormal Red Blood Cells and Diagnosing Specific Types of Anemia Using Image Processing and Support Vector Machine," *2019 IEEE 11th Int. Conf. Humanoid, Nanotechnology, Inf. Technol. Commun. Control. Environ. Manag. HNICEM 2019*, 2019.

[11] P. Tiwari *et al.*, "Detection of subtype blood cells using deep learning," *Cogn. Syst. Res.*, vol. 52, pp. 1036–1044, 2018.

[12] T. N. Kipf and M. Welling, "Semi-supervised classification with graph convolutional networks," *5th Int. Conf. Learn. Represent. ICLR 2017 - Conf.*

Track Proc., pp. 1–14, 2017.
[13] C. Y. Zhang, J. Hu, L. Yang, C. L. P. Chen, and Z. Yao, "Graph deconvolutional networks," *Inf. Sci. (Ny).*, vol. 518, pp. 330–340, 2020.
[14] J. Shi, R. Wang, Y. Zheng, Z. Jiang, H. Zhang, and L. Yu, "Cervical cell classification with graph convolutional network," *Comput. Methods Programs Biomed.*, vol. 198, p. 105807, Jan. 2021.
[15] T. N. Kipf and M. Welling, "Semi-Supervised Classification with Graph Convolutional Networks," *5th Int. Conf. Learn. Represent. ICLR 2017 - Conf. Track Proc.*, pp. 1–14, Sep. 2016.
[16] K. K. Jha, B. K. Das, and H. S. Dutta, "Detection of abnormal blood cells on the basis of nucleus shape and counting of WBC," *Proceeding IEEE Int. Conf. Green Comput. Commun. Electr. Eng. ICGCCEE 2014*, 2014.
[17] M. F. Syahputra, A. R. Sari, and R. F. Rahmat, "Abnormality classification on the shape of red blood cells using radial basis function network," *Proc. 2017 4th Int. Conf. Comput. Appl. Inf. Process. Technol. CAIPT 2017*, vol. 2018-Janua, no. April 2019, pp. 1–5, 2018.
[18] H. A. Aliyu, M. A. A. Razak, R. Sudirman, and N. Ramli, "A deep learning alexnet model for classification of red blood cells in sickle cell anemia," *IAES Int. J. Artif. Intell.*, vol. 9, no. 2, pp. 221–228, 2020.